Dental Materials Journal 23(4) : 504−511, 2004

Surface Properties of Electrochemically Buffed Titanium Casting

Seigo OKAWA, Awlad HOSSAIN, Mitsugu KANATANI, Kouichi WATANABE and Osamu MIYAKAWA
Division of Dental Biomaterial Science, Niigata University Graduate School of Medical and Dental Sciences, Gakkoucho-dori 2-5274, Niigata 951-8514, Japan
Corresponding author, E-mail:sokawa@dent.niigata-u.ac.jp

Received August 4, 2004/Accepted October 7, 2004

Electrochemical buffing, a combined process of electrochemical and mechanical polishing, was applied to titanium casting. Mixture of α-Al_2O_3 suspension (average grain diameter of 5 μm) and 5% KNO_3 solution was used as abrasive slurry. Specimen and experimental wheel buff were respectively connected to the positive and negative poles of a DC source, whose potential ratings ranged from 0 V (MEP) to 10 V (ECB10). Surface roughness, hardness, color, and cleanness were investigated. ECB10 surface produced a gold color and attained a mirror finish, as its roughness value was only one-quarter that of MEP. High amount of aluminum was present in MEP surface. Its bond state entirely differed from that of α-Al_2O_3, hence indicating surface alteration due to chemical reactions with the abrasive material. At higher potentials, reaction products might be dissolved anodically, so that the surface was chemically clean to some extent. The surface also became rich in OH^-.

Key words: Titanium, Polishing, Surface characterization

INTRODUCTION

Titanium has been used for various dental prostheses due to its excellent corrosion resistance and biocompatibility. For more extensive applications of titanium, attention has been focused on casting and welding techniques[1−4]. However, titanium has low thermal conductivity. This means that heat which is generated due to interactions with cutting tool does not dissipate quickly, which leads to temperature soaring high at cutting point. Under such conditions, tool is prone to react with inherently reactive titanium, hence undergoing severe chemical wear. Due to the chemical wear of tool, the machinability and grindability of titanium and its alloys pose a challenge[5−8]. To overcome this problem, some machinable titanium alloys have been developed in the dental field[9−11].

Similarly, titanium is not easy to mirror-finish. When conventional polishing techniques for dental alloys are applied to titanium, the surface tends to be satin-finished. Thus, other techniques, such as barrel polishing, electropolishing, and chemical polishing, have been noted and experimentally applied to titanium[12−16].

In barrel polishing, dental prosthesis is put into a barrel loaded with polishing chips. The barrel is subjected to mechanical movements. This method has relatively high polishing efficiency, but fails to create mirror surface for titanium[12]. Electropolishing of titanium has become feasible for the first time by using anhydrous electrolytes[13,14]. However, it is difficult to uniformly finish dental prostheses with complicated shapes, because electrochemical effect depends on the distance between workpiece surface and counter electrode[13]. In chemical polishing, titanium casting is pickled in solution containing hydrofluoric acid. However, we encountered difficulties in establishing the suitable conditions such as solution concentration, temperature, and pickling time[15], as well as in treatment of injurious chemical agents. Even if polishing is completed, metallic luster is poor and brightness does not last long[16].

On the other hand, in metal surface treatment field, Maehata *et al.* has devised an electrochemical buffing (ECB) process[17]. This process, in which anodic dissolution is combined with mechanical action of abrasive grains, has been successfully applied in final polishing of titanium. In dental applications, a similar method was experimentally applied to grind non-precious alloys[18,19].

In this study, ECB was applied to titanium casting to attain efficient finishing. For the purpose of comparison with mechanically polished surface, ECB-treated surfaces were characterized by means of surface roughness test, hardness test, electron probe microanalysis (EPMA), and X-ray photoelectron spectroscopy (XPS). The optimum condition for mirror finish was established and the applicability of ECB to titanium was evaluated.

MATERIALS AND METHODS

Preparation of specimen

Specimen was cast titanium plate of 13 mm in width, 40 mm in length, and 1.4 mm in thickness. In a dental titanium-casting unit (Titaniumer-VF, Ohara, Osaka, Japan), titanium ingot of JIS class 2 (Dental

Titanium, Ohara, Osaka, Japan) was cast into room temperature mold made from a phosphate-bonded investment (Titavest II, Ohara, Osaka, Japan). On a polishing machine (AUTOMAX, Refine Tech, Yokohama, Japan), both surfaces of specimen were abraded with waterproof abrasive papers of silicon carbide up to #800 grit under running tap water. Finally, specimen thickness was reduced to approximately 0.7 mm. Vickers hardness of abraded specimen showed a mean value of 170.3±7.4. Hence, the abrading process completely removed the reaction layers that had been formed on specimen surface through reactions with investment material components.

Electrochemical buffing unit

Fig. 1 shows a schematic diagram of the experimental setup, along with its external view. ECB unit was composed of three parts: specimen table driven by a stepping motor (103-540-0143, Sanyo Denki, Tokyo, Japan), experimental buffing wheel set in a straight handpiece (K-700, Morita, Kyoto, Japan), and a stabilized DC power source. Specimen was mounted on the table and then connected to the positive pole. The table was automatically reciprocated at 33 mm/min over a stroke of 25 mm in the longitudinal direction of specimen. Thus, the polished area was 13 (specimen width) × 25 (stroke length) mm^2.

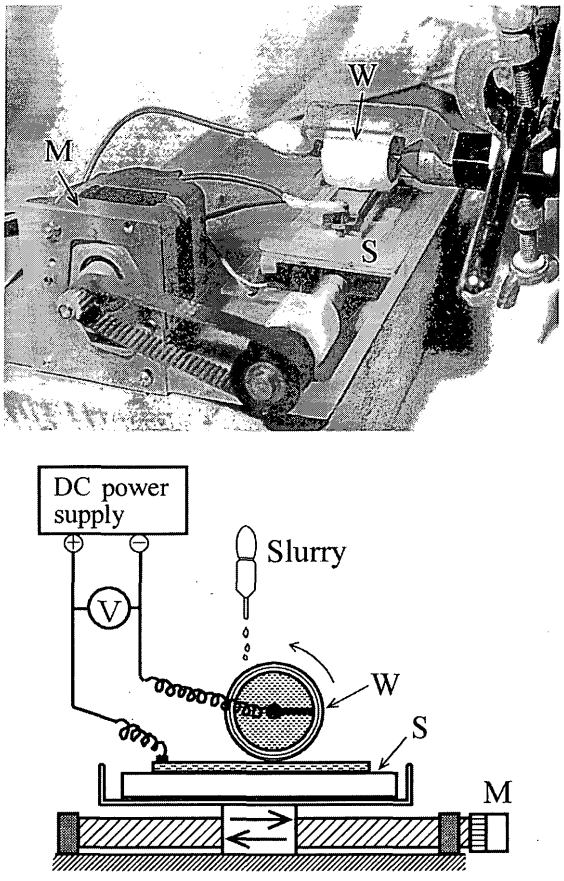

Fig. 1 Schematic diagram and external view of the experimental setup. ECB unit was composed of three parts: specimen table (S) driven by stepping motor (M), experimental buffing wheel (W) inserted into straight handpiece, and a stabilized DC power source.

For the experimental buffing wheel, a plastic cylinder, 23 mm in diameter and 25 mm in height, was mounted on a mandrel (PN250470, Pentron, Wallingford, CT, USA). The circumference of the cylinder was covered with platinum foil (Platinum Foil, Nihonbashi Tokuriki, Tokyo, Japan), which was doubly wrapped with a sheet of buffing cloth (Selvyt, Buehler, Lake Bluff, IL, USA). The foil was short-circuited to the mandrel, which was connected via a slip terminal to the negative pole. Wheel with fresh buffing cloth was used for each specimen.

The polishing load was set at approximately 300 g. At applied potentials of 0, 2, 4, 5, 6, 8, and 10 V, each specimen was polished for 600 s under intermittent dropping of abrasive slurry onto the rotating wheel. The rotation speed of the wheel was maintained at 2,000 rpm. After polishing, specimen was ultrasonically cleaned in acetone and then dried by air blow.

Preparation of abrasive slurry for ECB

An alumina suspension (average grain diameter: 5 μm) (No. 44-235, Refine Tech, Yokohama, Japan) was selected as the abrasive agent. According to X-ray diffractometry, the abrasive material proved to be α-Al_2O_3. With reference to a report by Furuno *et al.*[20], 5% solution of potassium nitrate (WAKO Pure Chem, Osaka, Japan) was prepared as electrolyte. The resultant abrasive slurry for ECB was a mixture of 50 ml of alumina suspension and 200 ml of electrolyte.

Material removal measurement

Before and after polishing, specimen was weighed on a direct-reading balance (L-II; Shimadzu, Kyoto, Japan). The weight difference was determined as "material removal". The mean of material removal and standard deviation were calculated from four specimens.

Surface roughness test

Centerline average roughness (Ra) was tested with a surface roughness tester (SURFCOM 100B, Tokyo Seimitsu, Mitaka, Japan) under the following conditions: cut-off value of 0.08 mm and measurement length of 10 mm. The mean of Ra and standard deviation were calculated from four specimens.

Hardness test

Four specimens were prepared for each condition. At two points randomly chosen on each specimen,

hardness was tested with a Micro Vickers hardness tester (MVK Type C, Akashi, Zama, Japan). The indentation load was 100 g and the retention time was 30 s. The mean hardness and standard deviation were obtained from the mean values of each specimen.

Surface analysis: EPMA

Secondary electron (SE) image of surface texture was taken using an electron probe microanalyzer (EPMA-8705 H-II, Shimadzu, Kyoto, Japan). For aluminum and oxygen distributions, an area equivalent to the image's was analyzed in sample stage scanning mode at an accelerating voltage of 15 kV and a specimen current of 0.3 μA.

Surface analysis: XPS

The polished surface, which underwent chemical alteration, was analyzed in an X-ray photoelectron spectrometer equipped with monochromated Al K_α excitation source (Quantum 2000, ULVAC-PHI, Chigasaki, Japan). High-resolution spectra, with pass energy of 58.70 eV, were acquired for C 1s, Al 2p, O 1s, and Ti 2p. The specimen chamber was held at a vacuum higher than 1.33 μPa. The analyzed area was 100 μm in diameter, and the take-off angle was 45°.

Ar^+ ion sputter etching and XPS analysis were alternately repeated, thereby determining the depth profiles of Al 2p, O 1s, and Ti 2p. The sputtered area was 2×2 mm^2. During sputtering, specimen was rotated to minimize the influence of surface unevenness on depth profile. The sputtering rates calibrated using silica as reference were 1.1 nm/min for the first 600 s sputtering, and then by 4.7 nm/min between 600 and 1,800 s. From the composition-depth profile of equal-thickness, multilayer SiO_2/TiO_2 half mirror, with which He-Ne laser oscillator was equipped, the sputtering rate of TiO_2 was estimated to be approximately half that of SiO_2. Accordingly, those rates for SiO_2, 1.1 and 4.7 nm/min, were converted into 0.6 and 2.4 nm/min for TiO_2, respectively. Hereinafter, the sputter-etched depth will be indicated by the value converted for TiO_2.

Since electrostatic surface charging leads to unexpected shift in binding energy, a neutralization gun was in operation during analysis. C 1s spectra from the outermost surface had a peak only at 284.8 eV, which was in accordance with the data of C-H or C-C bond available in published literature[21]. Thus, non-occurrence of peak shift was confirmed.

RESULTS

Surface morphology and color

Fig. 2 shows the SE images of polished surfaces at applied potentials of 0, 5, and 10 V, which are denoted by MEP, ECB5, and ECB10, respectively. In

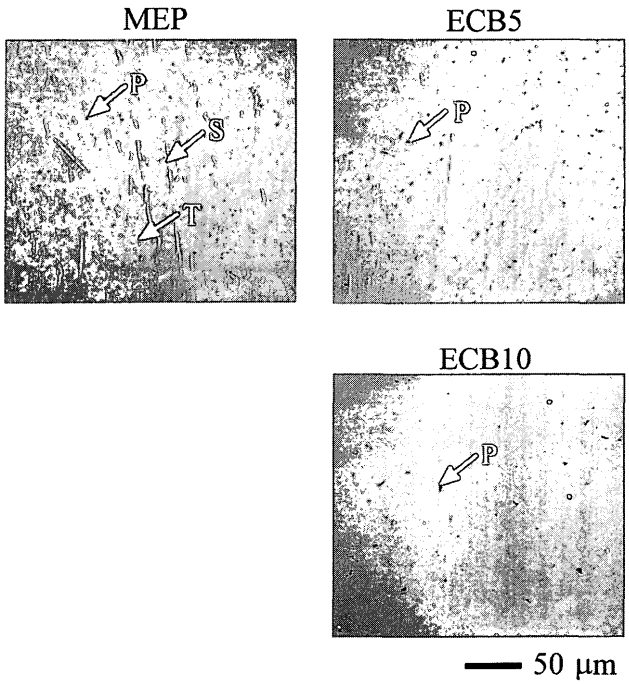

Fig. 2 SE images of polished surfaces at 0, 5, and 10 V (MEP, ECB5, and ECB10). A number of flaws of streak-type (S) and tear-type (T) were formed along the polishing direction of MEP. Small pits (P) were also observed. Flaws on ECB10 were rarely observed. Pits decreased in number and became slightly larger in size.

MEP without electrochemical effect, many flaws of streak- and tear-type were observed along the polishing direction, and small pits were randomly distributed. In ECB5, the number of streaks was reduced, which made pits clearly visible. In ECB10, hardly any flaw was observed. Although pits became slightly larger in size, the number of them decreased.

When polished at potentials of 5 V and above, the surface produced its color: whitish gold and gold for ECB5 and ECB10, respectively.

Applied potential versus material removal

At potentials of 0 to 4 V, the amount of material removal showed similar mean values ranging from 0.30 to 0.35 mg (Fig. 3). Assuming that the removed matter was composed of only titanium, the amounts were equal to 0.20 to 0.27 μm in thickness, respectively. In the region of 5 V, the mean value rose by approximately two times and thereafter kept at almost the same level.

Influence of applied potential on surface roughness and hardness

Surface roughness was remarkably improved in the range of 0 to 4 V, and thereafter the improvement

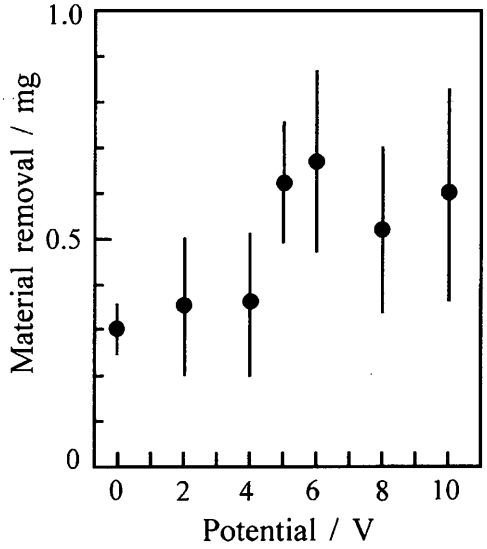

Fig. 3 Potential versus material removal. The material removal at 0 to 4 V showed similar mean values. In the region of 5 V, the mean value rose by approximately two times and thereafter kept at almost the same level.

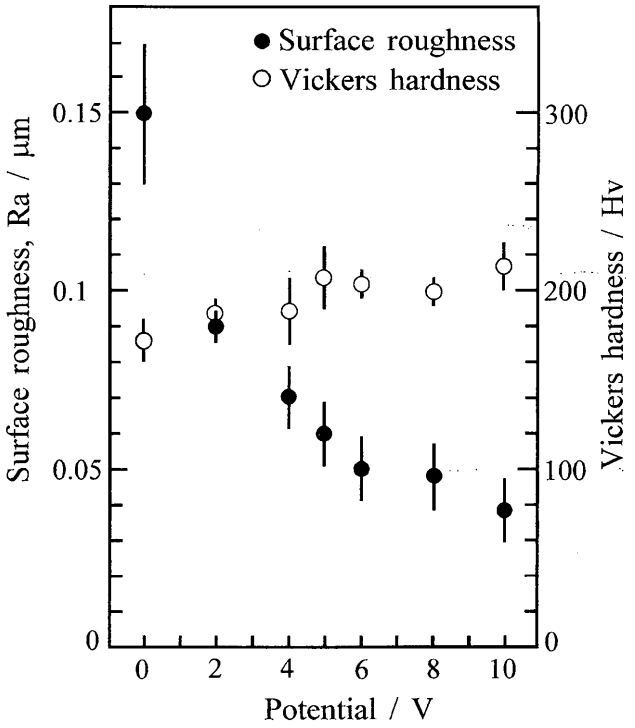

Fig. 4 Influences of potential on surface roughness and hardness. Surface roughness was remarkably improved in the range of 0 to 4 V and thereafter improved gradually. At 5 V and above, the hardness values were higher by about 10% than that of 0 V.

became gradual (Fig. 4). Ra value was $0.15 \pm 0.02 \mu m$ for MEP, finally decreasing to $0.04 \pm 0.01 \mu m$ for ECB10.

ECB surfaces tended to harden. In particular at potentials of 5 V and above, the hardness values were higher by about 10% than that of MEP (Fig. 4).

EPMA

In MEP surface, high amounts of aluminum and oxygen were present with non-uniform distributions (Fig. 5). The observed non-uniformity might partly result from surface unevenness, as the directions normal to abraded slopes were different from point to point with respect to the location of each element detector.

In ECB5 surface, slight positional variation of aluminum concentration was still found, but the whole averaged level fell below EPMA's detection limit. On the contrary, oxygen concentration reached a higher averaged level, while keeping a remarkable positional variation.

In ECB10 surface, like that of ECB5, the aluminum signal showed a background level, except for a few peaks. In contrast, oxygen was uniformly distributed with a high averaged level, except for the aluminum-rich points. In summary, MEP surface was rich in aluminum and oxygen, whereas ECB reduced aluminum amount and enhanced oxygen amount.

XPS

In Fig. 6, Al 2p depth profiles of MEP are compared against those of ECB10. All spectra showed unsymmetrical profiles, hence indicating the presence of two or more aluminum-containing compounds in both surfaces. For the outermost surface, both spectra were located on binding energy side higher than 73.7 eV assigned to Al^{3+} of α-Al_2O_3. As sputtering time increased, both spectra were further shifted to high energy side. When comparing the corresponding spectra at the same depth, the signal intensity from MEP was much higher than that from ECB10. Moreover, the signal from more inner depth was able to be detected in MEP. This could be partly due to difference in surface unevenness between MEP and ECB10.

O 1s spectra (Fig. 7) from both the outermost surfaces had two major components at 530.5 eV (Ti-O bond) and 531.7 eV (O-H bond)[22,23]. But the amount of OH^- was higher on ECB10 surface than

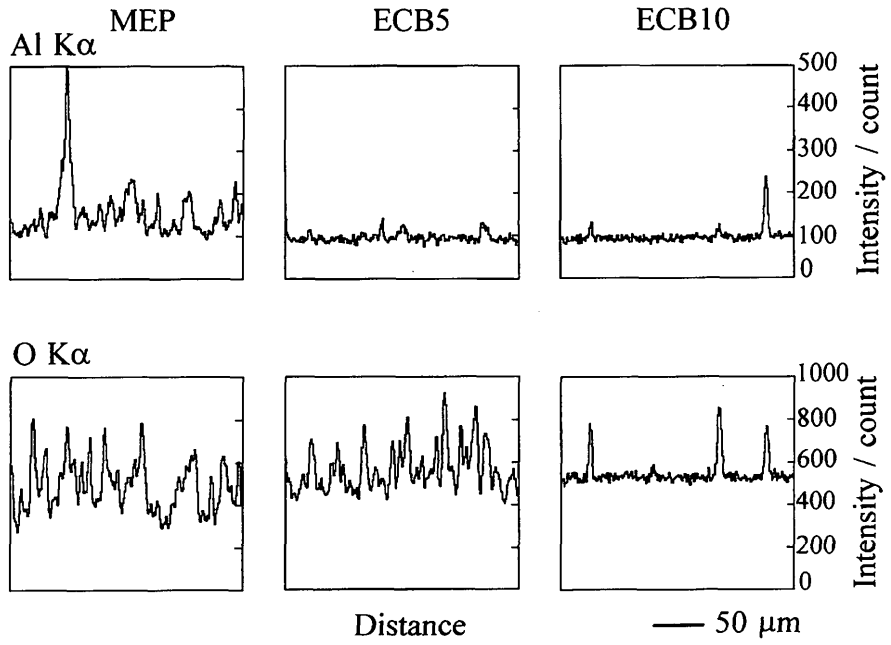

Fig. 5 Line profiles of Al K_α and O K_α intensities. The profiles are depicted along the horizontal midline of SE images shown in Fig. 2. In MEP surface, Al and O with high amounts were present, whereas ECB reduced Al amount and enhanced O amount.

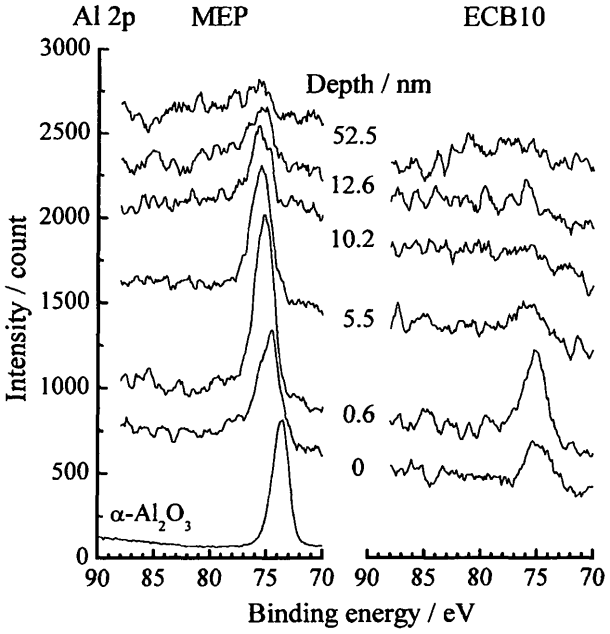

Fig. 6 Depth profiles of Al 2p for MEP and ECB10. Sputtered depth is indicated as value converted for TiO_2. All spectra suggested the presence of two or more Al-containing compounds in both surfaces. The signal intensity from MEP was much higher than that from ECB10.

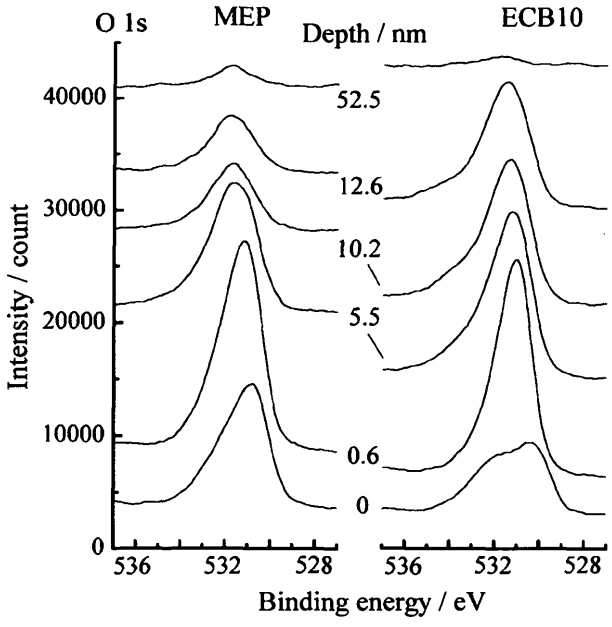

Fig. 7 Depth profiles of O 1s for MEP and ECB10. Sputtered depth is indicated as value converted for TiO_2. The spectra from both the outermost surfaces suggested the presence of two major bonds at 530.5 eV (Ti-O bond) and 531.7 eV (O-H bond). The OH^- amount was higher on ECB10 than on MEP.

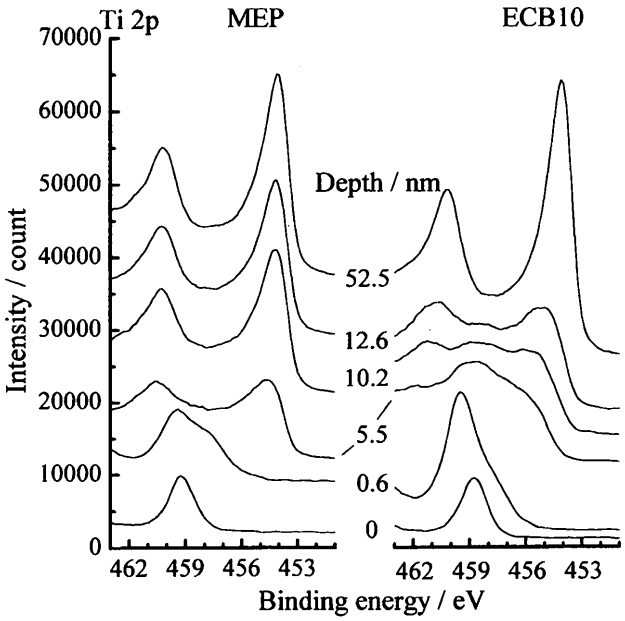

Fig. 8 Depth profiles of Ti 2p for MEP and ECB10. Sputtered depth is indicated as value converted for TiO_2. At depth shallower than 5.5 nm, MEP surface already disclosed Ti^0 $2p_{3/2}$ peak at 454.1 eV. But ECB10 surface eventually showed a similar peak profile when sputter-etched at 10-12 nm depth.

on MEP surface. At the same sputtering depth, the integrated intensity of O 1s spectrum was higher for ECB10 than for MEP.

Initially, Ti $2p_{3/2}$ spectra corresponded to titanium oxides (Fig. 8). At depth shallower than 5.5 nm (converted depth for TiO_2), MEP surface already disclosed another peak at 454.1 eV, which corresponded to metallic titanium[24]. As for ECB10 surface, it eventually showed a similar peak profile when sputter-etched at 10-12 nm depth. These results, coupled with O 1s data, indicated that the oxide layer on ECB10 surface was much thicker than that on MEP surface.

DISCUSSION

Mechanism of creating mirror surface

In general, electropolishing anodically smoothens metal surface in electrolyte[25]. Since higher density current flows into electrolyte from protruded surface than from hollow surface, protruded portions are preferentially dissolved and removed. In this way, surface becomes gradually smooth with electropolishing time.

During electropolishing, a film of metallic salt or oxide forms on the metal surface. Meanwhile, the metal continues to dissolve in electrolyte until the film grows to a dense, stable layer that can protect the metal from anodic dissolution[25]. The same is almost true with titanium. The main difference is that the titanium surface is naturally covered with a stable oxide layer which offers excellent protection.

In ECB, however, the action of abrasive grain is also at work. Since the sharp grain edge mechanically destroys the oxide layer, fresh titanium substrate itself is momentarily exposed to electrolyte. Therefore, even at potentials lower than 4 V, anodic dissolution should occur for a short time until oxide regenerates through anodic oxidation and grows to be a stable layer. Through the aid of mechanical abrasion, anodic dissolution can play an important role in improving surface roughness. In the range of 0 to 4 V, this hypothetical inference reasonably accounts for the remarkable decrease in roughness value without significant increase in material removal (Fig. 4).

At potentials of 5 V and above, amount of material removal rose by approximately two times (Fig. 3). Two possible factors are presumed for this rise. First, higher potentials brought about breakdown of the oxide layer, thus promoting anodic dissolution of substrate titanium. For titanium, the passive range extends over a potential range of several volts. Depending on the titanium alloy, the breakdown (or pitting) potential in 20% NaCl solution at 20℃, for example, lies between 3 and 8 V[26]. The other factor was surface hardening due to anodic oxidation, which will be discussed in detail later. In abrading relatively soft metals with large plasticity, as is the case with titanium, surface is apt to be plowed by abrasive grain. Since pieces of plowed material are put aside, this plowing phenomenon interferes with the formation of abrading chips, significantly lowering the abrading efficiency. Thus, the slight hardening at higher potentials (Fig. 4) might inhibit the plowing phenomenon to some extent and facilitate the formation of abrading chips. However, it is difficult to quantitatively discriminate between the abrading and dissolving effects on material removal.

Relatively small pits were observed on polished surfaces (Fig. 2). Most likely, the pits were formed at the end of abrasion streaks where abrasive particles suddenly stopped fast running. Most pits were removed by anodic dissolution as well as by mechanical abrasion. The remaining pits grew slightly at higher potentials, because the relative dissolution rate within and outside the pit was different[25].

Anodic oxidation

Coloring at higher potentials results from interference of light in the oxide layer thickened by anodic oxidation. The results of EPMA (Fig. 5) and XPS (Figs. 7-8) were consistent with the hypothesis that the oxide layer becomes thick due to anodic oxidation. The surface was immediately colored at the location where buffing wheel passed. The color was not changed when buffing was repeated. In other

words, coloring was dependent on applied potential but independent of ECB time. A linear relationship between applied potential and oxide layer thickness has been reported together with anodic oxidation coloring[27]. Although the relationship between both quantities depends on anodizing conditions, color has one-to-one correspondence to oxide layer thickness. With reference to the reported data[27], the oxide layer thickness on ECB10 surface with gold color was estimated to be roughly 10 nm. This estimation was supported by fairly good agreement with the present XPS data (Fig. 8).

One prerequisite condition for oxide layer to increase its thickness along with potential is that the oxide layer should have high ionic conductivity[28]. Thus, the oxide layer formed by ECB is assumed to have a structure in which ions are allowed to diffuse easily.

In general, hardness reflects the mechanical property that is averaged throughout the depth range of several tens to several hundreds of micrometers. Therefore, the increase in oxide layer thickness by only a few nanometers seems to be too small to account for the surface hardening found in the present study (Fig. 4). Detailed Rutherford backscattering study of the anodically oxidized surface below breakdown limit has demonstrated that the transition from oxide to metal is able to extend two to three times its nominal thickness into the metal[29]. This suggests oxygen dissolution in the metal with a large diffusion coefficient. Titanium is known to harden remarkably with increasing concentration of solute oxygen[30]. Therefore, the dissolution of oxygen in the extended transition may give a reasonable explanation for the slightly increased hardness.

Cleanness of polished surface

Abrasive materials such as Al_2O_3 and Fe_2O_3 usually contaminate the abraded or polished surface with constituents of the abrasive material[31,32]. The reason is that in abrading or polishing, these abrasive materials come into direct contact with native titanium, which is inherently reactive with most elements. As a result, reaction products are left in the regenerated oxide layer. In the present study, aluminum concentration in MEP surface, which underwent only mechanical abrasion, was much higher than that in ECB surface (Fig. 5).

Therefore, the objective of XPS was to investigate whether titanium reacted similarly with abrasive material. The chemical bond state of aluminum present in the polished surfaces was entirely different from that of Al^{3+} in α-Al_2O_3 (Fig. 6). Therefore, the embedment of abrasive grains into the surface could not account for the alteration of surface composition. Probably, the abrasive material reacted with titanium and left behind reaction products such as $Ti_xAl_yO_z$ and $Ti_xAl_y(OH)_z \cdot nH_2O$ in the regenerated oxide layer. Further investigation is needed to identify these products.

On the other hand, ECB created a relatively clean surface (under the detection limit of EPMA), although XPS detected a small amount of aluminum. Inferentially, the cleanness resulted from anodic dissolution of reaction products.

ECB-modified surface was rich in chemical species of OH^- (Fig. 7). Therefore, the surface may have special surface characteristics such as electrostatic charge, wettability, and protein adsorption. Further investigations are needed to elucidate the characteristics and biocompatibility of ECB surface.

CONCLUSIONS

Electrochemical buffing was applied to titanium casting in a potential range of 0 to 10 V. Slurry mixture of α-Al_2O_3 suspension (average grain diameter of 5 μm) and 5% KNO_3 solution was used.

As potential was raised to 5 V, surface roughness was remarkably improved without significant increase in material removal. Thereafter, the amount of material removal rose by about two times, but roughness improved only gradually. The surface was colored and slightly hardened due to anodic oxidation. At 10 V, the surface produced a gold color and attained a mirror finish with centerline average roughness of 0.04 ± 0.01 μm. Reaction products between titanium and the abrasive material were formed in the mechanically polished surface. However, at 10 V, these products were hardly detected, probably because they were anodically dissolved.

When compared to the mechanically polished surface, the electrochemically buffed surface was rich in chemical species of OH^-.

ACKNOWLEDGEMENTS

The authors are grateful to Mr. S. Nakano and Mrs. H. Honma, technicians in the Dental Biomaterial Science division, for their respective assistances in preparing specimens and collecting reference materials. The authors are also grateful to Mr. M. Kobayashi, operator of EMX Laboratory, Niigata University Center for Instrumental Analysis, for his helpful suggestions and assistance in element analysis.

REFERENCES

1) Nakai A. Study of resin-bonded calcia investment. Part 2: Effect of titanium content on the dimensional change of the investment. Dent Mater J 2002; 21: 191-199.
2) Fujioka S, Kakimoto K, Inoue T, Okazaki J, Komasa Y. Metallurgical effects on titanium by laser welding on dental stone. Dent Mater J 2003; 22: 581-591.
3) Meng Y, Nakai A, Goto S, Ogura H. Study of resin-

bonded calcia investment. Part 3: Hardness of titanium castings. Dent Mater J 2004; 23: 46-52.
4) Sato H, Komatsu M, Miller B, Shimizu H, Fujii H, Okabe T. Mold filling and microhardness of 1% Fe titanium alloys. Dent Mater J 2004; 23: 211-217.
5) Miyakawa O, Watanabe K, Okawa S, Kanatani M, Nakano S, Kobayashi M. Surface contamination of titanium by abrading treatment. Dent Mater J 1996; 15: 11-21.
6) Takahashi M, Kikuchi M, Takada Y, Okuno O. Mechanical properties and microstructures of dental cast Ti-Ag and Ti-Cu alloys. Dent Mater J 2002; 21: 270-280.
7) Hotta Y, Miyazaki T, Fujiwara T, Tomita S, Shinya A, Sugai Y, Ogura H. Durability of tungsten carbide burs for the fabrication of titanium crowns using dental CAD/CAM. Dent Mater J 2004; 23: 190-196.
8) Takahashi M, Kikuchi M, Okuno O. Mechanical properties and grindability of experimental Ti-Au alloys. Dent Mater J 2004; 23: 203-210.
9) Kikuchi M, Takahashi M, Okuno O. Mechanical properties and grindability of dental cast Ti-Nb alloys. Dent Mater J 2003; 22: 328-342.
10) Kikuchi M, Takahashi M, Okabe T, Okuno S. Grindability of dental cast Ti-Ag and Ti-Cu alloys. Dent Mater J 2003; 22: 191-205.
11) Kikuchi M, Okuno O. Machinability evaluation of titanium alloys. Dent Mater J 2004; 23: 37-45.
12) Miyazaki T, Tamaki Y, Tanaka H, Aoyama N. The effect of variation in volume of chips in a barrel on the polishing properties of titanium by the centrifugal barrel polishing. J Showa Univ Dent Soc 1994; 14: 164-170.
13) Morita N. Study of pure titanium electrolytic polishing. J Jpn Dent Mater 1990; 9: 218-238.
14) Piotrowski O, Madore C, Landolt D. Electropolishing of titanium alloys in perchlorate-free electrolytes. Plating & Sur Fin 1998; 5: 115-119.
15) Tamaki Y, Miyazaki T, Suzuki E, Miyaji T. Polishing of titanium prosthetic. Part 4: Chemical polishing. J Jpn Dent Mater 1988; 7: 786-791.
16) Japan titanium society. Processing technology of titanium, Nikkan Kogyo Shinbunsya, Tokyo, 1992, p.188.
17) Maehata H, Kamada H, Yamamoto M. A study on the electrolytic-abrasive mirror finishing. J Jpn Soc Prec Eng 1985; 51: 136-143.
18) Tamaki Y. Electro-mechanical grinding of dental alloys. J Jpn Dent Mater 1986; 5: 804-811.
19) Kyo K, Ohmori H, Okamoto Y. Characteristic of mirror surface grinding of dental nickel-titanium alloy using ELID (electrolytic in-process dressing). Int J Jpn Soc Prec Eng 1998; 32: 183-187.
20) Furuno T, Uchihira T, Usuku T. Study on electrolytic grinding of cemented carbide. J Jpn Metal Fin Soc 1966; 17: 6-12.
21) Moulder JF, Stickle WF, Sobol PE, Bomben KD. Handbook of X-ray photoelectron spectroscopy, Physical Electronics Inc, Minnesota, 1995, p.216.
22) Shibata T, Zhu YC. The effect of film formation conditions on the structure and composition of anodic oxide films on titanium. Corros Sci 1995; 37: 253-270.
23) Sul YT, Johansson CB, Petronis S, Krozer A, Jeong Y, Wennerberg A, Albrektsson T. Characteristics of the surface oxides on turned and electrochemically oxidized pure titanium implants up to dielectric breakdown: the oxide thickness, micropore configurations, surface roughness, crystal structure and chemical composition. Biomater 2002; 23: 491-501.
24) Moulder JF, Stickle WF, Sobol PE, Bomben KD. Handbook of X-ray photoelectron spectroscopy, Physical Electronics Inc, Minnesota, 1995, p.240.
25) Landolt D. Fundamental aspects of electropolishing. Electrochem Acta 1987; 32: 1-11.
26) Brunette DM, Tengvall P, Textor M, Thomsen P. Titanium in Medicine, Springer, Berlin, 2001, p.154-162.
27) Japan titanium society. Processing technology of titanium, Nikkan Kogyo Shinbunsya, Tokyo, 1992, p.191.
28) Ohtsuka T, Masuda M, Sato N. Ellipsometric study of anodic oxide films on titanium in hydrochloric acid, sulfuric and phosphate solution. J Electrochem Soc 1985; 132: 787-792.
29) Serroys Y, Sakout T, Gorse D. Anodic oxidation of titanium in 1M H_2SO_4, studied by Rutherford backscattering. Sur Sci 1993; 282: 279-287.
30) Collings EW. The physical metallurgy of titanium alloys, American society for metals, Ohio, 1984, p.141.
31) Miyakawa O, Okawa S, Kobayashi M, Uematsu K. Surface contamination of titanium by abrading treatment. Dent in Jpn 1998; 34: 90-96.
32) Akhter R, Okawa S, Nakano S, Kobayashi M, Miyakawa O. Surface composition and structure of titanium polished with aqueous slurry of ferric oxide. Dent Mater J 2000; 19: 10-21.